Spectral dynamics of square pulses in passively mode-locked fiber lasers

Georges Semaan,[1,*] Andrey Komarov,[2] Alioune Niang,[1] Mohamed Salhi,[1] and François Sanchez[1]
[1]*Laboratoire de Photonique d'Angers EA 4464, Université d'Angers, 2 Boulevard Lavoisier, 49000 Angers, France*
[2]*Institute of Automation and Electrometry, Russian Academy of Sciences, Acad. Koptyug Prospekt 1, 630090 Novosibirsk, Russia*

(Received 11 October 2017; published 6 February 2018)

We investigate experimentally and numerically the spectral dynamics of square pulses generated in passively mode-locked fiber lasers under the dissipative soliton resonance. The features of the transition from the single-peak spectral profile to the doublet spectrum with increasing pump power are studied. The used master equation takes into account the gain saturation, the quadratic frequency dispersion of the gain and the refractive index, and the cubic-quintic nonlinearity of the losses and refractive index. Experimental data are obtained for an Er:Yb-doped fiber ring laser. The theoretical and experimental results are in good agreement with each other.

DOI: 10.1103/PhysRevA.97.023812

I. INTRODUCTION

Over the last two decades, passively mode-locked fiber lasers had been extensively investigated because of the high demand for compact, cheap, and precise laser technology in many practical applications such as biomedicine, industrial micromachining, and defense [1,2]. One of the important advantages of these lasers despite their different applications is the great variety of their operating regimes under different mode-locking mechanisms—nonlinear polarization evolution or nonlinear optical loop mirrors. In fact, they can operate with a single pulse in a laser cavity and in multiple pulse regimes [3]. In the anomalous dispersion, multiple pulsing is possible due to the energy quantization. This allows the formation of various soliton distributions such as two-soliton molecules with different phase differences for the soliton amplitude [4] and multisoliton complex analogous to different states of matter (soliton gas, liquid, rain, and crystal) [5]. Also, multiple pulse operation can be implemented as a harmonic passive mode-locking regime [6], in which the distance between all neighboring pulses in the laser cavity is identical. Passively mode-locked fiber lasers exhibit various hysteresis phenomena, bistabilities, and multistabilities (bistability between a continuous wave and mode-locked or Q-switched regimes, the dependence of the number of identical solitons in the laser cavity, or the soliton shape on the initial lasing conditions) [7]. Achieving high pulse intensities in all-fiber soliton configurations has always been difficult because of different limiting factors such as distortion and multipulsing instabilities. In fact, the effect of the energy quantization is the key obstacle to the generation of high-energy pulses. In the anomalous dispersion fiber laser, increasing the pump power increases the number of pulses in the laser cavity so that the upper energy limit of an individual pulse is fixed by the pulse duration and the cavity parameters. Dissipative soliton generation can be achieved if the balance between dispersion and nonlinearities is available, and loss is balanced by gain [8,9]. To circumvent these problems, novel operational modes and strategies have been developed [10,11]. The phenomenon of dissipative soliton resonance remains one of the most interesting beam-shaping techniques used since it allows the energy to increase linearly with the pulse width inside the cavity. Based on the complex cubic-quintic Ginzburg-Landau equation, it shows that the soliton energy increases indefinitely with specific parameters while keeping the peak power stable at a certain level [12–14]. Komarov *et al.* [6] have demonstrated that the increase of the pulse width leads to a decrease of its spectral width, which may be responsible for the suppression of multipulse operation and the stabilization of the single pulse. Square pulses have been experimentally observed in normal and anomalous dispersion regimes [15–22]. Experimental results have shown that long fiber cavities promote the generation of energetic square pulses operating under dissipative soliton resonance [23]. Different spectral dynamics of dissipative soliton resonance square pulses have been experimentally reported. In [21], a single-lobe spectral profile was observed regardless of the pump power, whereas in [24], whatever the pump power, it consisted of a double-lobe spectrum profile. A dual spectral peak was first mentioned in a numerical study [25] where the authors did not investigate it in detail. Recently, the stability of a single square pulse and the spectral changes were thoroughly investigated in an anomalous dispersion for specific parameters of the fiber laser cavity [26]. The generation of stable square pulses with a spectral doublet structure by increasing the pump power has been reported numerically. In [19], the study focused on maximizing the energy of dissipative soliton resonance (DSR) pulses in a fiber ring cavity. The corresponding reported double-lobe spectrum was nearly independent of the pump power for high pumping rates. Therefore, a numerical study on square pulses with spectral doublet profile was considered in [26]. It was demonstrated that under certain cavity conditions, such spectral profile contributes to the stability of the square pulses. The reported theoretical results confirm, as experimentally reported in [19], that the distance between the spectral peaks was nearly constant. However, the analysis in both numerical and experimental cases was limited to high pumping rates well above the threshold. Thus, it would be interesting to consider

*Corresponding author: georges.semaan@univ-angers.fr

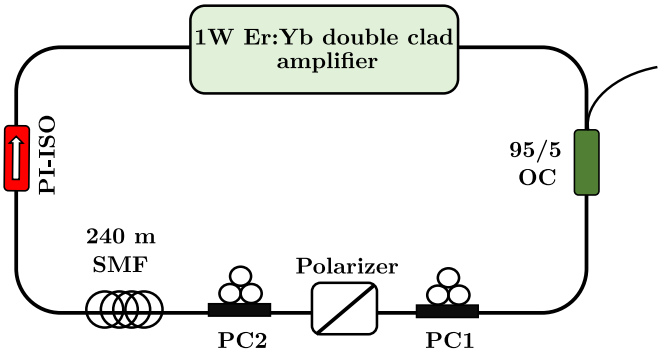

FIG. 1. Experimental setup of the nonlinear polarization evolution: PI-ISO (polarization-insensitive isolator), PC (polarization controller), and OC (output coupler).

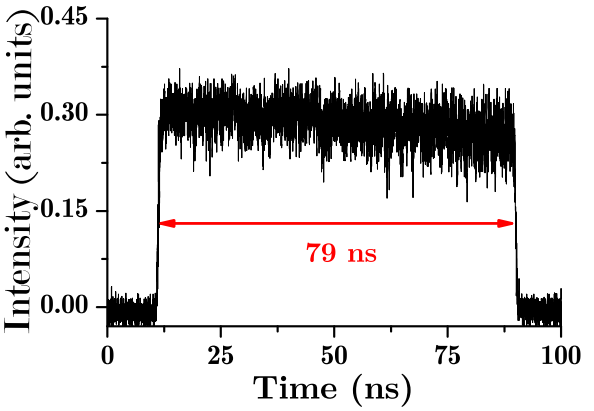

FIG. 2. Temporal profile of the laser emission registered at 633 mW of pump power.

the region in which the transition from a single-lobe spectrum at the threshold [26,27] to spectral doublets as a function of the pump power occurs. The main objective of this paper is to investigate the spectral dynamics of square pulses in fiber ring cavities, where we point out experimentally and theoretically the interplay between the temporal and spectral characteristics of the pulses. The paper is organized as follows. In Sec. II, we present the experimental schematic for the fiber laser cavity in the anomalous dispersion regime. Experimental results are discussed in Sec. III. Section IV gives a theoretical analysis of the experimental results based on a complex cubic-quintic nonlinear equation. The basic conclusions are made in Sec. V.

II. EXPERIMENTAL SETUP

The experimental schematic of the fiber laser setup is presented in Fig. 1. It is based on a simple all-fiber ring cavity configuration operating under the nonlinear polarization evolution mode-locking mechanism. We use a C-band double-clad V-groove Er:Yb 1.2 W fiber amplifier from Keopsys. The amplifier is pumped by several laser diodes operating at 980 nm delivering up to 5 W. The 3-m-long double-clad fiber has a second-order dispersion of $\beta_2 = -0.021$ ps^2 m^{-1}. To ensure the DSR operation, we built a large anomalous dispersion cavity by splicing a piece of 240 m single-mode fiber (SMF). The total cavity length is about 250 m, including 247 m of SMF with a second-order dispersion of $\beta_2 = -0.022$ ps^2 m^{-1} and the net cavity dispersion is about $\beta_2 L = -5.49$ ps^2. Two polarization controllers (PC) were used with an inline polarizer to operate under the nonlinear polarization evolution mode-locking mechanism. A polarization-insensitive isolator (PI-ISO) was also employed. An output coupler is used to extract 5% of the power from the cavity. The output intensity is measured using a high-speed photodetector (TIA-1200) and visualized with a fast oscilloscope (Tektronix TDS 6124C, 12 GHz, 40 GSs^{-1}). Also, the output power is measured using a high-power integrating sphere (Thorlabs S146C). The spectral properties are analyzed with an optical spectrum analyzer (Anritsu MS 9710C).

III. EXPERIMENTAL RESULTS

To start, we adjust the cavity parameters to obtain square pulses. When the polarization controllers' paddles are properly fine tuned, square-wave mode-locked pulses are observed at the output of the laser for a pump power above 400 mW. Figure 2 shows the typical pulses generated by the laser at 633 mW of pump power. The laser delivers square pulses with 78 ns pulse width. If the polarization controllers are altered during the experiment, we observe other regimes such as multiple square pulses [28]. Stability is revealed through the radio-frequency spectrum (rf) shown in Fig. 3, which points out a signal-to-noise ratio around 50 dB. The repetition frequency of the constructed laser is around 800 kHz, which corresponds to a 250-m-long cavity. Although the main purpose is to examine the spectral dynamics of the square pulses rather than demonstrating the generation of DSR pulses [19,20,28], we have checked, nevertheless, that the laser operates effectively in the DSR regime [19–23]. The graph depicted in Fig. 4 confirms that both pulse energy and width can be linearly tuned with the pump power, while maintaining a relatively stable peak power. The achieved pulse tuning ranges from 23 to 79 ns, and the pulse energy from 12 to 37.5 nJ by taking into consideration a repetition frequency of 800 kHz. The peak power is clamped around 0.55 W. According to Komarov [26], stable square pulses with a spectral doublet can be achieved in fiber lasers and the pulse-width tuning and energy scaling are determined

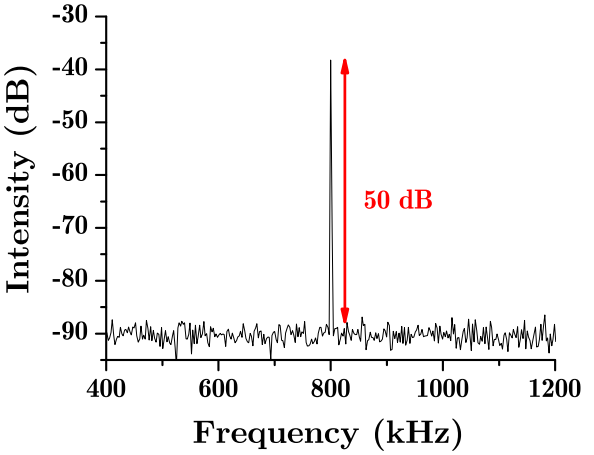

FIG. 3. The rf spectrum registered with 100 Hz BW at 633 mW of pump power.

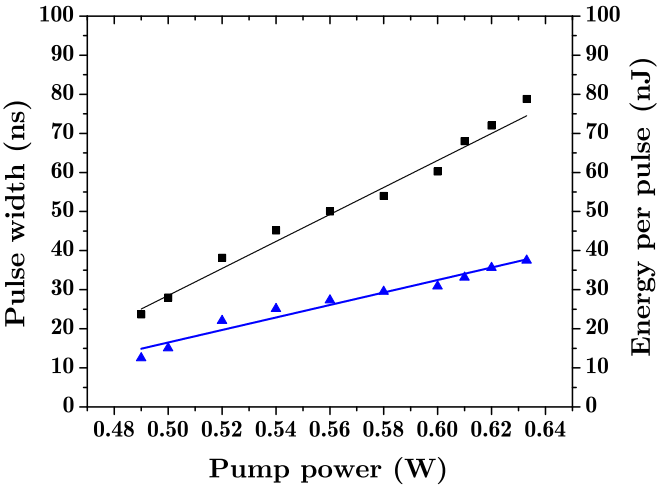

FIG. 4. Pulse width (black squares) and pulse energy (blue triangles) as a function of pump power.

by the spectral dynamics. In fact, it has been demonstrated that while increasing the pump power in the anomalous dispersion regime, the spectral width of the doublets decreases while the position remains unchanged. The latter has been observed experimentally in [19]. As stated in Sec. I, here we focus on the spectral dynamics near threshold. Figure 5 exhibits the spectral profile of the laser emission as a function of the pump power from the threshold to about 30% above threshold. Results show that in contrast with experimental [19] and theoretical results [24], the spectrum progressively evolves from a single-lobed to double-lobed profile. Indeed, at 490 mW pump power, the spectrum is centered on 1587 nm with a bandwidth at 3 dB of 3 nm, while at 633 mW, the spectrum has two lobes centered at 1566 and 1602 nm. The 3 dB bandwidth of each lobe is 1.2 and 5.3 nm, respectively. The transition is smooth and continuous. Experimental results also show that the distance between the two spectral lobes tends to a constant value for high pumping rates, as reported in [19]. The corresponding temporal profile is depicted in Fig. 6, where the pulse width is tuned from 23 to 79 ns.

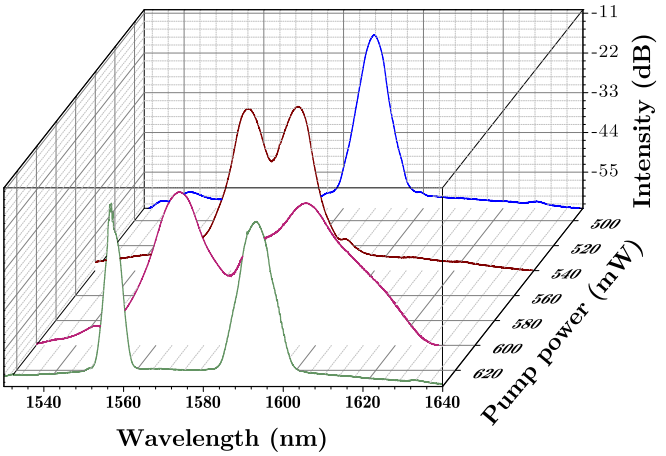

FIG. 5. Spectral profile of the square pulse for various values of the pump power.

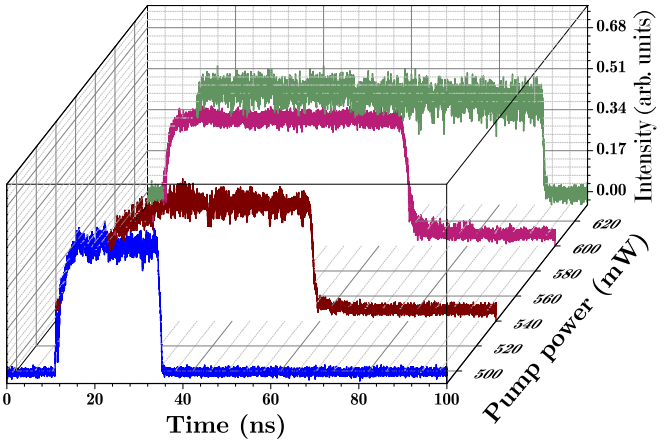

FIG. 6. Temporal profile of the square pulse as a function of the pump power.

To highlight the spectral evolution, we present the variation in the spectral spacing between the two spectral lobes as a function of pumping power. Results given in Fig. 7 show that the spectral spacing continuously varies from zero (single-lobed spectrum) to higher values. Experimental data seem to suggest a linear increase of the spectral spacing but, as demonstrated in Sec. IV, the spacing saturates to a constant value for higher pumping rates. Experimental constraints prevent us from further increasing the pumping power, but such constant saturation was shown in an independent experiment [19].

IV. NUMERICAL RESULTS

We aim to investigate theoretically the spectral dynamics of a fiber laser operating in the DSR regime near the lasing threshold. Our analysis is based on the normalized complex equation with cubic-quintic nonlinearity, which describes the field evolution in a unidirectional ring laser with a uniformly

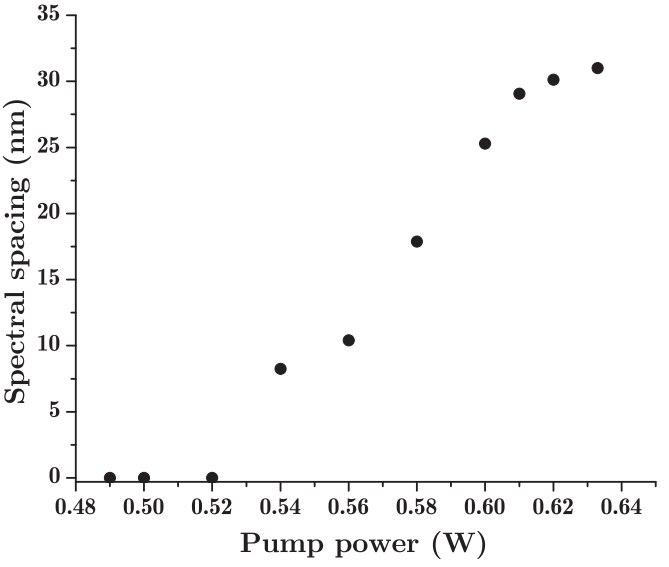

FIG. 7. Spectral spacing evolution as a function of pump power.

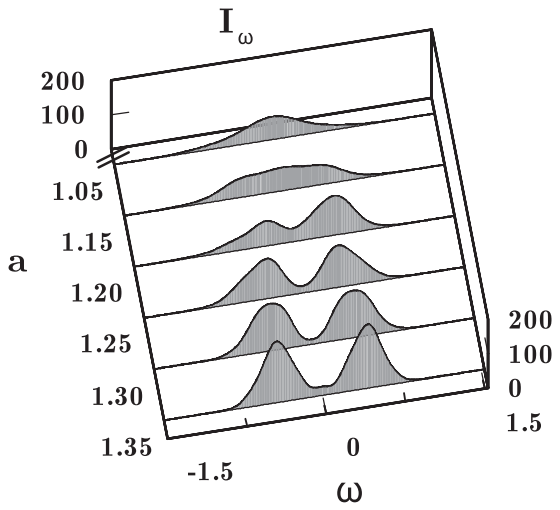

FIG. 8. Spectral $I_\omega(\omega)$ profile of a steady-state pulse as a function of the pump power a. $b = 0.02$, $D = 0.5$, $D_i = 0$, $q = 0.4$, $\sigma_0 = 1$, $p = 1$, and $p_2 = 1$.

distributed intracavity medium [24],

$$\frac{\partial E}{\partial \zeta} = (D_r + iD_i)\frac{\partial^2 E}{\partial \tau^2} + [g + (p + iq)I - p_2 I^2]E, \quad (1)$$

where $E(\zeta,\tau)$ is the electric-field amplitude, τ is the time coordinate in units $\delta\tau = \sqrt{|\beta_2|\frac{L}{2}}$ (here β_2 is the second-order group-velocity dispersion for the intracavity medium and L is the cavity length), ζ is the normalized propagation distance (the number of passes of the radiation through the laser cavity), D_r and D_i are the frequency dispersions of the gain and of the refractive index, respectively, and q is the cubic nonlinearity of the refractive index. The term $g = a/(1 + b\int I d\tau) - \sigma_0$ is the total amplification including the linear losses σ_0 (here the integration is carried out over the whole round-trip period), a is the pumping parameter, and b is the saturation parameter. The variable g is normalized by dividing the corresponding dimensional variable by the dimensional linear losses. The terms p and p_2 are the cubic and quintic nonlinearities of

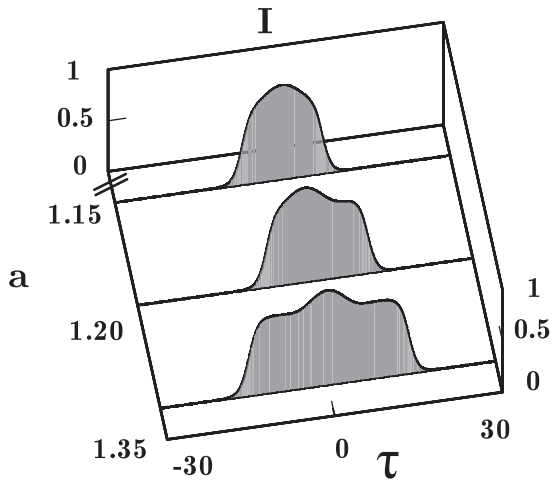

FIG. 9. Temporal $I(\tau)$ profile of a steady-state pulse as a function of the pump power a. $b = 0.02$, $D = 0.5$, $D_i = 0$, $q = 0.4$, $\sigma_0 = 1$, $p = 1$, and $p_2 = 1$.

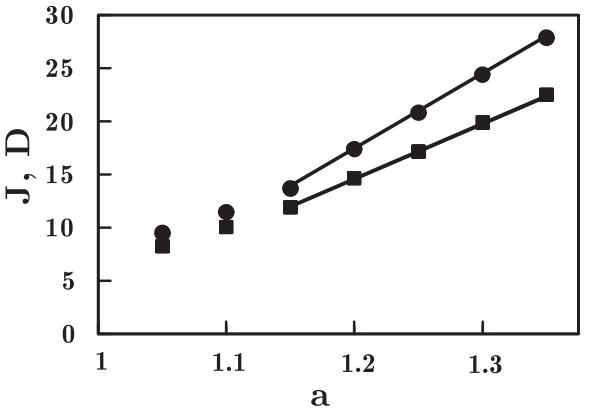

FIG. 10. Dependences of the duration D (black circles) and energy J (black squares) of the steady-state pulse on the pump power a.

losses ($p > 0, p_2 > 0$) and $I = |E|^2$ is the field intensity in units γL^{-1}, where γ (W^{-1} m^{-1}) is the dimensional nonlinear refractive coefficient related to the nonlinear refractive index. The growth in the peak intensity of pulses is limited by the nonlinearity p_2.

The results of the numerical simulation for the spectral $I_\omega = I_\omega(\omega)$ and temporal $I = I(\tau)$ profiles of the steady-state pulse are shown in Figs. 8 and 9. By increasing the pump power, the bell-shaped spectral profiles are transformed into a spectral doublet, and the bell-shaped temporal profile is transformed into a square profile. In the neighborhood of $a = 1.2$, solutions with symmetric distributions $I_\omega(\omega)$ and temporal $I(\tau)$ are unstable. Therefore, states with asymmetric distributions of intensity and spectrum are realized. There is a one-to-one correspondence between two spectral peaks in Fig. 8 and two parts of a rectangular pulse in Fig. 9, which are separated from each other by a small peak located on a square pulse. Asymmetry in the spectrum at $a = 1.2$ means the displacement of this peak from the center of the square pulse. When square pulses (symmetrical or asymmetrical) are generated, the dependences of the duration D and energy J of the steady-state pulse are linear functions of the pump power a (see Fig. 10). This fact means the continuity of the peak intensity of a square pulse under change of the pump power. Figure 11 shows the distance D_ω between the spectral peaks

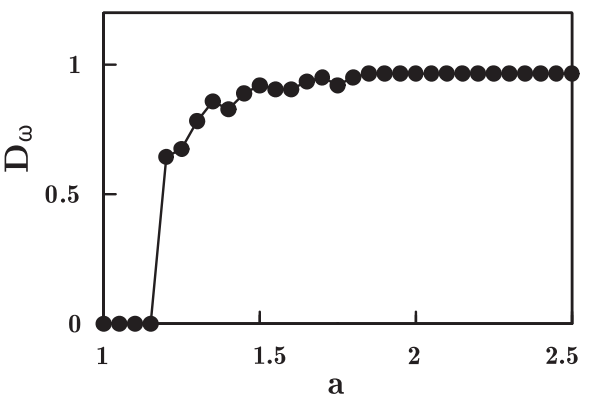

FIG. 11. Distance D_ω between the spectral peaks in a spectral doublet of a steady-state pulse as a function of the pump power a.

in a spectral doublet of a steady-state pulse as a function of the pump power a. With sufficiently large pump power $a > 1.7$, this distance becomes constant. The obtained numerical results are in good qualitative agreement with the experimental results. Indeed, near threshold the distance between the spectral peaks increases, as experimentally reported in Sec. III, while for higher pumping powers, this distance is nearly constant, as previously observed in [19]. The obtained results show that the spectral doublet is caused by the self-action of the square pulse in a nonlinear intracavity medium and not by linear spectral selection of radiation due to intracavity losses with two spectral maxima of transmission.

V. CONCLUSION

In conclusion, we have investigated the spectral dynamics of a Er:Yb-doped fiber ring laser operating in the DSR regime near the lasing threshold. The generated square pulses present a spectral-doublet structure that is influenced by the change of pump power. We demonstrated that the optical spectrum continuously varies from a bell-shaped to a double-lobed profile. This evolution is accompanied by a linear increase of the square-pulse duration. Experimental results have been theoretically modeled thanks to a cubic-quintic master equation. Numerical simulations are in good qualitative agreement with experimental data.

[1] C.-J. Chen, P. Wai, and C. Menyuk, Opt. Lett. **17**, 417 (1992).
[2] M. E. Fermann and I. Hartl, Nat. Photon. **7**, 868 (2013).
[3] A. Grudinin, D. Richardson, and D. Payne, Electron. Lett. **28**, 67 (1992).
[4] N. N. Akhmediev, A. Ankiewicz, and J. M. Soto-Crespo, Phys. Rev. Lett. **79**, 4047 (1997).
[5] F. Amrani, A. Haboucha, M. Salhi, H. Leblond, A. Komarov, and F. Sanchez, Appl. Phys. B **99**, 107 (2010).
[6] A. Komarov, F. Amrani, A. Dmitriev, K. Komarov, and F. Sanchez, Phys. Rev. A **87**, 023838 (2013).
[7] D. Tang, W. Man, and H. Tam, Opt. Commun. **165**, 189 (1999).
[8] W. H. Renninger, A. Chong, and F. W. Wise, JOSA B **27**, 1978 (2010).
[9] N. Akhmediev, in *General Theory of Solitons*, edited by A. D. Boardman and A. P. Sukhorukov, Soliton-Driven Photonics (Kluver Academic Publishers, Netherlands, 2001), pp. 371–395.
[10] F. W. Wise, A. Chong, and W. H. Renninger, Laser Photon. Rev. **2**, 58 (2008).
[11] W. H. Renninger, A. Chong, and F. W. Wise, IEEE J. Sel. Top. Quantum Electron. **18**, 389 (2012).
[12] N. Akhmediev, J. M. Soto-Crespo, and P. Grelu, Phys. Lett. A **372**, 3124 (2008).
[13] W. Chang, A. Ankiewicz, J. M. Soto-Crespo, and N. Akhmediev, Phys. Rev. A **78**, 023830 (2008).
[14] W. Chang, J. M. Soto-Crespo, A. Ankiewicz, and N. Akhmediev, Phys. Rev. A **79**, 033840 (2009).
[15] X. Wu, D. Tang, H. Zhang, and L. Zhao, Opt. Express **17**, 5580 (2009).
[16] L. Duan, X. Liu, D. Mao, L. Wang, and G. Wang, Opt. Express **20**, 265 (2012).
[17] X. Zhang, C. Gu, G. Chen, B. Sun, L. Xu, A. Wang, and H. Ming, Opt. Lett. **37**, 1334 (2012).
[18] Z.-C. Luo, W.-J. Cao, Z.-B. Lin, Z.-R. Cai, A.-P. Luo, and W.-C. Xu, Opt. Lett. **37**, 4777 (2012).
[19] G. Semaan, F. B. Braham, M. Salhi, Y. Meng, F. Bahloul, and F. Sanchez, Opt. Express **24**, 8399 (2016).
[20] G. Semaan, F. B. Braham, J. Fourmont, M. Salhi, F. Bahloul, and F. Sanchez, Opt. Lett. **41**, 4767 (2016).
[21] K. Krzempek, Opt. Express **23**, 30651 (2015).
[22] K. Krzempek, J. Sotor, and K. Abramski, Opt. Lett. **41**, 4995 (2016).
[23] K. Krzempek and K. Abramski, Opt. Express **24**, 22379 (2016).
[24] T. Liu, D. Jia, Y. Liu, Z. Wang, and T. Yang, Opt. Commun. **356**, 416 (2015).
[25] P. Grelu, W. Chang, A. Ankiewicz, J. M. Soto-Crespo, and N. Akhmediev, JOSA B **27**, 2336 (2010).
[26] A. Komarov, A. Dmitriev, K. Komarov, D. Meshcheriakov, and F. Sanchez, Phys. Rev. A **94**, 043827 (2016).
[27] A. Komarov, A. Dmitriev, K. Komarov, D. Meshcheriakov, G. Semaan, and F. Sanchez, Phys. Rev. A **96**, 033820 (2017).
[28] G. Semaan, A. Niang, M. Salhi, and F. Sanchez, Laser Phys. Lett. **14**, 055401 (2017).